Propulsion and Power Research 2020;xxx(xxx):1−11

http://ppr.buaa.edu.cn/

Propulsion and Power Research

www.sciencedirect.com

ORGINAL ARTICLE

Galerkin finite element analysis of magneto-hydrodynamic natural convection of Cu-water nanoliquid in a baffled U-shaped enclosure

A. Zaim[a], A. Aissa[b], F. Mebarek-Oudina[c,d,*], B. Mahanthesh[e], G. Lorenzini[f], M. Sahnoun[b], M. El Ganoui[g]

[a]*BLSTE Laboratory, Faculty of Science and Technology, University of Mascara, Mascara, Algeria*
[b]*Laboratoire de Physique Quantique de La Matière et Modélisation Mathématique (LPQ3M), Université Mustapha Stambouli de Mascara, Mascara, Algeria*
[c]*Department of Physics, Faculty of Sciences, University of 20 Août 1955-Skikda, Skikda, 2100, Algeria*
[d]*Laboratoire des Matériaux et Génie Energétique (LMGE), University of 20 Août 1955-Skikda, Skikda, 2100, Algeria*
[e]*Department of Mathematics, CHRIST (Deemed to Be University), Bangalore, 560029, India*
[f]*Department of Engineering and Architecture, University of Parma, Parco Area Delle Scienze 181/A, 43124, Parma, Italy*
[g]*Laboratoire énergétique de Longwy (FJV/LERMAB), Université de Lorraine, France*

Received 25 February 2020; accepted 18 October 2020
Available online XXXX

KEYWORDS

Natural convection;
Nanoliquid;
Rayleigh number;
Baffled U-shaped;
Nusselt number;
Galerkin finite element method

Abstract In this paper, single-phase homogeneous nanofluid model is proposed to investigate the natural convection of magneto-hydrodynamic (MHD) flow of Newtonian Cu−H_2O nanoliquid in a baffled U-shaped enclosure. The Brinkman model and Wasp model are considered to measure the effective dynamic viscosity and effective thermal conductivity of the nanoliquid correspondingly. Nanoliquid's effective properties such as specific heat, density and thermal expansion coefficient are modeled using mixture theory. The complicated PDS (partial differential system) is treated for numeric solutions via the Galerkin finite element method. The pertinent parameters Hartmann number ($1 \leq Ha \leq 60$), Rayleigh number ($10^3 \leq Ra \leq 10^6$) and

*Corresponding author.
E-mail addresses: oudina2003@yahoo.fr, f.mebarek_oudina@univ-skikda.dz (F. Mebarek-Oudina).
Peer review under responsibility of Beihang University.

Production and Hosting by Elsevier on behalf of KeAi

https://doi.org/10.1016/j.jppr.2020.10.002

nanoparticles volume fraction ($0\% \leq \phi \leq 4\%$) are taken for the parametric analysis, and it is conducted via streamlines and isotherms. Excellent agreement between numerical results and open literature. It is ascertained that heat transfer rate enhances with Rayleigh number *Ra* and volume fraction ϕ, however it is diminished for larger Hartmann number *Ha*.

Nomenclature

B	applied magnetic field (unit: Tesla)
k	thermal conductivity (unit: W/(m·K))
H	height of the enclosure (unit: m)
h	length of the baffle (unit: m)
Ha	Hartmann number
Nu	Nusselt number
Pr	Prandtl number
Ra	Rayleigh number
T	fluid temperature (unit: K)
U, V	dimensionless velocity components
W	weight of enclosure (unit: m)
X	position of the baffle (unit: m)

Greek letters

α	thermal diffusivity (unit: m^2/s)
β	thermal expansion coefficient (unit: 1/K)
θ	dimensionless temperature
ρ	density (unit: kg/m^3)
σ	electrical conductivity (unit: S/m)
μ	dynamic viscosity (unit: kg/(m·s))
ϕ	volume fraction (unit: %)

Subscripts

avg	average
c	cold
f	fluid
h	hot
Local	local
nf	nanofluid
s	solid particle

1. Introduction

The study of free convection heat transfer involving nanoliquids has achieved immense consideration among the researchers in recent years because of its various implications in many areas, including heat exchangers, cooling of electronic devices, industrial machines, chemical treatment equipment and solar collectors. With a chief objective of develop superior heat transport functioning liquids with a superior thermal diffusivity, several numeric and semi-analytic methods were employed to study the behavior of nanoliquids in natural convection [1,2]. The significance of magnetism in a square cavity with natural convection by utilizing gallium liquid was analyzed by Sathiyamoorthy and Chamkha [3]. They showed that the average number of Nusselt decreases with the inclination angles, in a non-linear way as the number of Hartmann increases. Mahmoudi et al. [4] used copper-water nanofluid for cooling a heat source fixed to the vertical wall of a square cavity. Their results indicate that heat transfer can be improved by reducing the length of the heater and increasing the nanoparticles volume fraction for a defined heater geometry at a given Rayleigh number.

Free convection heat transfer of Titania nanofluid in a cylindrical annulus with heater and various base fluids was analyzed in Ref. [5]. The influence of ϕ, *Ra* and the base fluid kinds on the thermal efficiency was discussed. The heat transfer of TiO_2 nanofluids intensifies with boosting ϕ at various *Ra* and the choose of the base fluid. Al-Najem et al. [6] proved that the potency of an inclination angle and magnetism had an apparent cause on the flow characteristics and the heat transfer mode. Khan et al. [7] modeled a hybrid nanofluid comprising nanometric materials through an ethylene glycol, where the magnetic impact on the convective flow is revealed with the impacts of Joule heating and viscous dissipation. The reliability and stability of the obtained results are classified with the stability analysis. Magnetic number slows velocity and temperature distribution in the first solution (FS), while they found the opposite behavior in the second solution (SS). Among studies that are relevant to this area, we cite also that of Öztop et al. [8] where they conducted a numerical study on natural convection in a chamber with two semi-circular heating elements on the lower wall. They found a significant influence of the distance between hot springs on the thermal regime, with a negative effect of the Hartmann number. Other studies have been carried out on magneto hydrodynamics, especially on entropy generation [9,10] and forced convection.

With the aim of control the flow of fluids and improve thermal performance, several approaches and techniques have been proposed such as: the use of porous media [10,11], fins [12], the corrugated walls [13], and the magnetic field [14−17].

Irreversibility in convection heat transfer of Newtonian Cu-water nanofluid in an enclosure with chamfers was investigated for various parameters as *Pr* and *Ra* numbers in Ref. [9]. It was shown that the growth of *Ra* number have a weak importance for reducing thermal irreversibility. At a

fixed tilt angle of the magnetic field, irreversibility increases for small Hartman number and reaches a maximum value at the critical moment (Ha_c) then it decreases.

Moreover, many studies reported on the heat transfer performance of non-Newtonian nanofluid [18,19] where the impact of various variable parameters are used.

We can model the heat transfer of the nanofluids either by the single-phase method where the nanofluid is modeled as a homogeneous mixture of nanoparticles and base liquid or by a two-phase method, in which the nanoparticles and the base liquid are treated as phases distinct with distinct patterns for each phase; therefore it is assumed that the base fluid and the nanoparticles have different velocity and temperature fields. The single-phase model under predicts convective heat transfer coefficient whereas the two-phase models provide more accurate prediction of this coefficient with an overestimation [20–22].

Sayehvand et al. [23] investigated numerically the ordinary convection of Al_2O_3 nanoliquid in a square cavity with partitions. Their results established that the Nusselt number and Rayleigh number are proportional directly, however, the Nusselt number negatively correlated with baffle length. Medebber et al. [24] have also proved that the Nusselt number and Rayleigh number are proportional directly though their investigation of heat transport in cylindrical annular enclosure filled with nanoliquid. Their results concluded that solid concentration is positively correlated with Nusselt number. Numerical study was presented by Kandaswamy et al. [25] to investigate the buoyancy convection in baffles. Their results drawn conclusion that length of baffle is favourable for higher heat transfer rate.

Armaghani et al. [26] analyzed the baffle length causes in natural convection of nanofluid with entropy generation in baffled L-shaped cavity. Ma et al. [27] presented numerical analysis to study ordinary convection in a U-shaped baffled enclosure by involving nanoliquids. Zuo et al. [28] deliberated the influence of baffles on pressurization and thermal stratification in cryogenic tanks under micro-gravity. They found that with two annular baffles installed, the pressurization is mitigated by the existence of baffles. The problem of heat transport in heated square cavity which is differentially heated is studied by Saravanan et al. [29] by considering heat generating two baffles. Recently, Ma et al. [30] used lattice Boltzmann scheme to investigate the nanofluids ordinary convection in baffled U-shaped enclosure. Benzenine et al. [31] performed a comparative study numerically among two models of baffles such as rectangular and trapezoidal planes. Their result indicates that the trapezoidal baffles guarantee a considerable augment of the velocity compared to the rectangular baffles but with an increase in friction. Entropy analysis of CuO–H_2O nanoliquid is carried out by Chamkha et al. [32] in a C-shaped cavity under magnetic field and they obtained that entropy production rate increased due to the presence of nanoparticles.

There is still no study in the literature on the natural convection of nanofluids in U-shaped enclosures with two baffles. The reason for this study is the service of non-square magnetic field developers and technical cooling sensors for electronic devices. Since the natural convection of nanofluids in thermal applications will broaden current knowledge, a numerical study is being conducted on the Maxwell nanofluid load with Cu in a U-shaped enclosure equipped with a baffle using the FEM method. The effects of Ra, Ha, and ϕ on the flow system and heat transfer properties are also examined.

2. Problem statement

Let us take two-dimensional U-shaped enclosure filled with magneto nanoliquid as shown (Figure 1). The bottom wall is maintained at high and constant temperature (T_h) and middle walls of square (5,6,7,8) are cold (T_c). The baffle is made of highly conductive material; the temperature of the baffle is imposed at the same temperature of the wall (T_c) which it is attached.

The governing dimensionless equations for mass, momentum, and energy in a medium are given respectively by:

$$\frac{\partial U}{\partial X}+\frac{\partial V}{\partial Y}=0, \tag{1}$$

$$U\frac{\partial U}{\partial X}+V\frac{\partial U}{\partial Y}=-\frac{\partial P}{\partial X}+\frac{\mu_{nf}}{\rho_{nf}\alpha_f}\left(\frac{\partial^2 U}{\partial X^2}+\frac{\partial^2 U}{\partial Y^2}\right), \tag{2}$$

$$U\frac{\partial V}{\partial X}+V\frac{\partial V}{\partial Y}=-\frac{\partial P}{\partial Y}+\frac{\mu_{nf}}{\rho_{nf}\alpha_f}\left(\frac{\partial^2 V}{\partial X^2}+\frac{\partial^2 V}{\partial Y^2}\right)+\frac{(\rho\beta)_{nf}}{\rho_{nf}\beta_f}RaPr\theta - Ha^2PrV, \tag{3}$$

$$U\frac{\partial \theta}{\partial X}+V\frac{\partial \theta}{\partial Y}=\frac{\alpha_{nf}}{\alpha_f}\left[\frac{\partial^2 \theta}{\partial X^2}+\frac{\partial^2 \theta}{\partial Y^2}\right]. \tag{4}$$

All the symbols are defined in the nomenclature section. The effective nanoliquid properties are modeled using mixture theory and phenomenological laws. Now, the density of nanoliquid is given by Brinkman [33]:

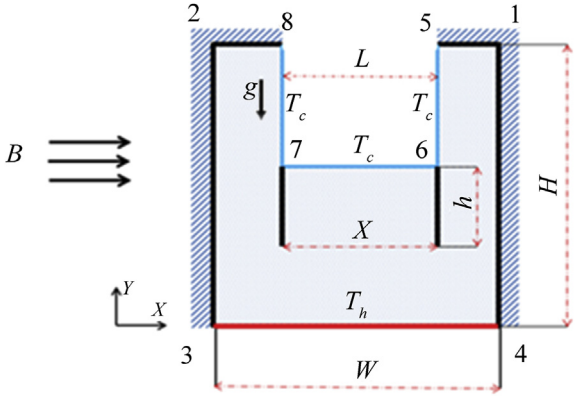

Figure 1 Physical model and coordinate system.

Table 1 The properties of Cu and H_2O [9].

	ρ/(kg/m^3)	C_p/(J/(kg•K))	K/(W/(m•K))	σ/(S/m)	β/(K^{-1})
H_2O	997.1	4179	0.613	5.5×10^{-5}	21×10^{-5}
Cu	8933	385	401	59.6×10^{-5}	1.67×10^{-5}

$$\rho_{nf} = \rho_f(1-\phi) + \rho_s\phi, \tag{5}$$

The specific heat capacity can be determined according to Pak and Cho [34].

$$(\rho C_p)_{nf} = (\rho C_p)_f(1-\phi) + (\rho C_p)_s\phi, \tag{6}$$

The coefficient of thermal expansion is given as Brinkman [33]:

$$\beta_{nf} = \beta_f(1-\phi) + \beta_s\phi, \tag{7}$$

The effective dynamic viscosity based on the Brinkman model is considered as Brinkman [33]:

$$\mu_{nf} = \frac{\mu_f}{(1-\phi)^{2.5}}, \tag{8}$$

Thermal conductivity is defined as [5]:

$$\frac{k_{nf}}{k_f} = \frac{(k_s - 2k_f) - 2\phi(k_f - k_s)}{(k_s - 2k_f) + \phi(k_f - k_s)}, \tag{9}$$

For the thermal conductivity [9,35]:

$$\frac{\sigma_{nf}}{\sigma_f} = 1 + \frac{3\left(\frac{\sigma_s}{\sigma_f} - 1\right)\phi}{\left(\frac{\sigma_s}{\sigma_f} + 2\right) - \left(\frac{\sigma_s}{\sigma_f} - 1\right)\phi}, \tag{10}$$

The values of thermo-physical properties for different materials are displayed in Table 1, Brinkman [33].

Dimensionless Eq. (1)−(4) are obtained by applying following non-dimensional parameters,

$$X = \frac{x}{W}, Y = \frac{y}{Y}, U = \frac{uW}{\alpha_f}, V = \frac{vW}{\alpha_f}, P = \frac{pW^2}{\rho_{nf}\alpha_f^2}, \theta = \frac{T - T_c}{T_h - T_c}. \tag{11}$$

$$Ra = \frac{g\beta_f H^3(T_h - T_c)}{\alpha_f \nu_f}, \tag{12}$$

$$Pr = \frac{\nu_f}{\alpha_f}, \tag{13}$$

$$Ha = B_0 W\sqrt{\frac{\sigma_f}{\rho_f \nu_f}}, \tag{14}$$

The local Nusselt number and the average value at the hot wall are obtained as:

Table 2 Average Nusselt number Nu_{avg} comparison for different grid resolution.

Case	Name	Mesh size	Nu_{avg}
1	Coarse	225	6.2250
2	Normal	529	6.9018
3	Fine	841	7.1072
4	Finer	1296	7.2281
5	Extra finer	5929	7.3898
6	Extremely fine	22,500	7.3998

$$Nu_{avg} = \frac{1}{W}\int_0^W Nu_{Local}dX|_{Y=0}, \tag{15}$$

where

$$Nu_{Local} = -\frac{k_{nf}}{k_f}\frac{\partial\theta}{\partial Y}\bigg|_{Hot\ wall}. \tag{16}$$

3. Numerical solution

The nonlinear PDS (partial differential system) was treated by employing the Galerkin finite element method (see Refs. [36,37] for more details). This method consists of converting nonlinear differential equations into an arrangement of integral expressions. Non-uniform triangular grids were employed in the discretization of the field's solution. Several references are available in the literature to solve this system of equations using analytical or numerical methods as [38,39]. Mesh testing technique adapted to pledge the grid-independency of the obtained solution. We have examined six divorce grid forms with 225, 529, 841, 1296, 5929 and 22,500 numbers of elements within the resolution

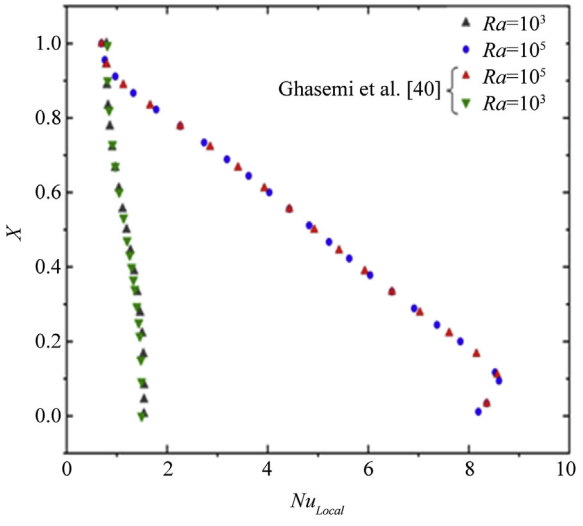

Figure 2 Physical comparison of the local Nusselt number Nu_{Local} at different Rayleigh number Ra when $Ha = 0$ with numerical data of Ghasemi et al. [40].

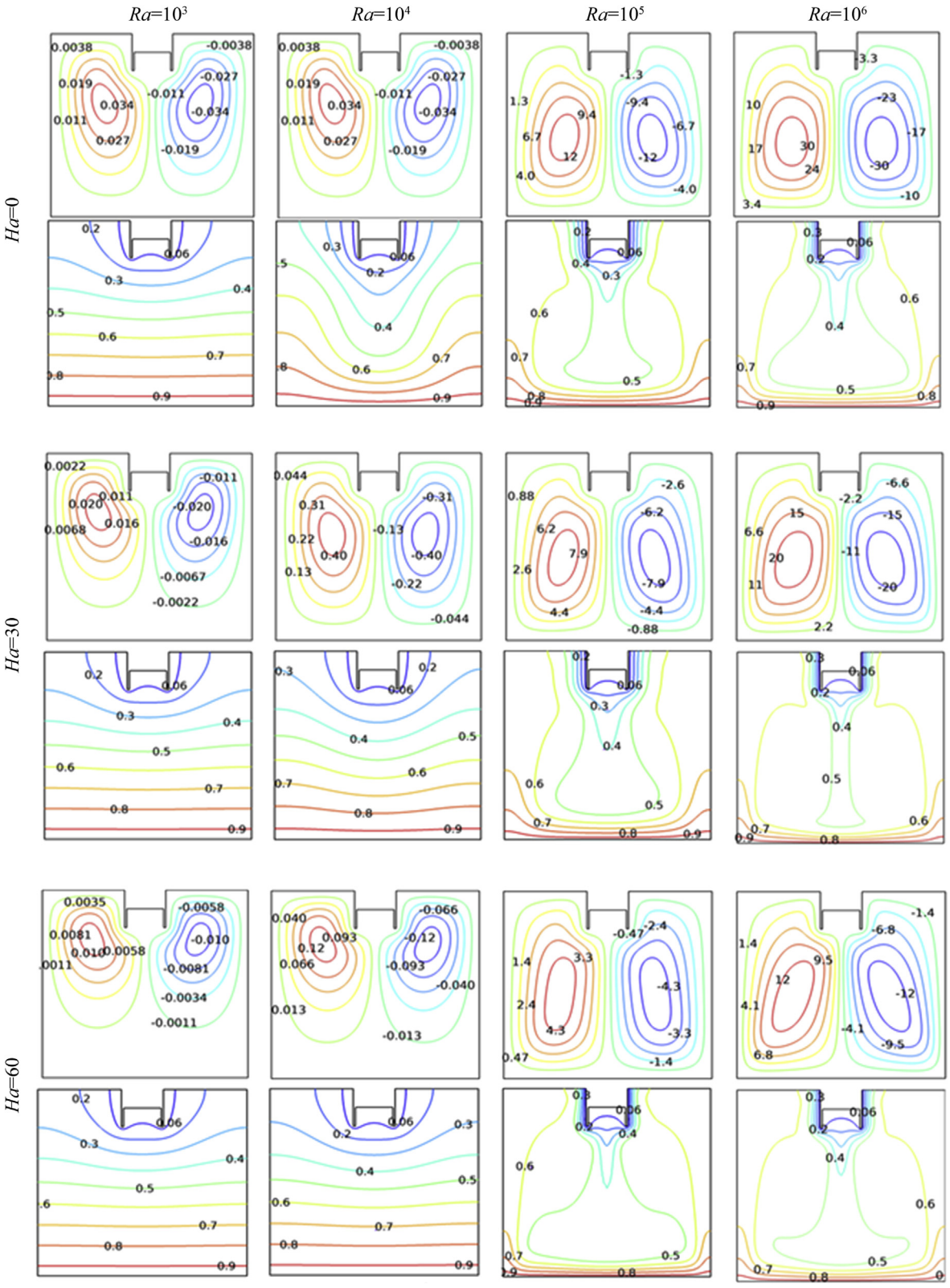

Figure 3 Influence of Rayleigh number *Ra* and Hartmann number *Ha* on streamlines and isotherms at nanoparticle volume fraction $\phi = 0$.

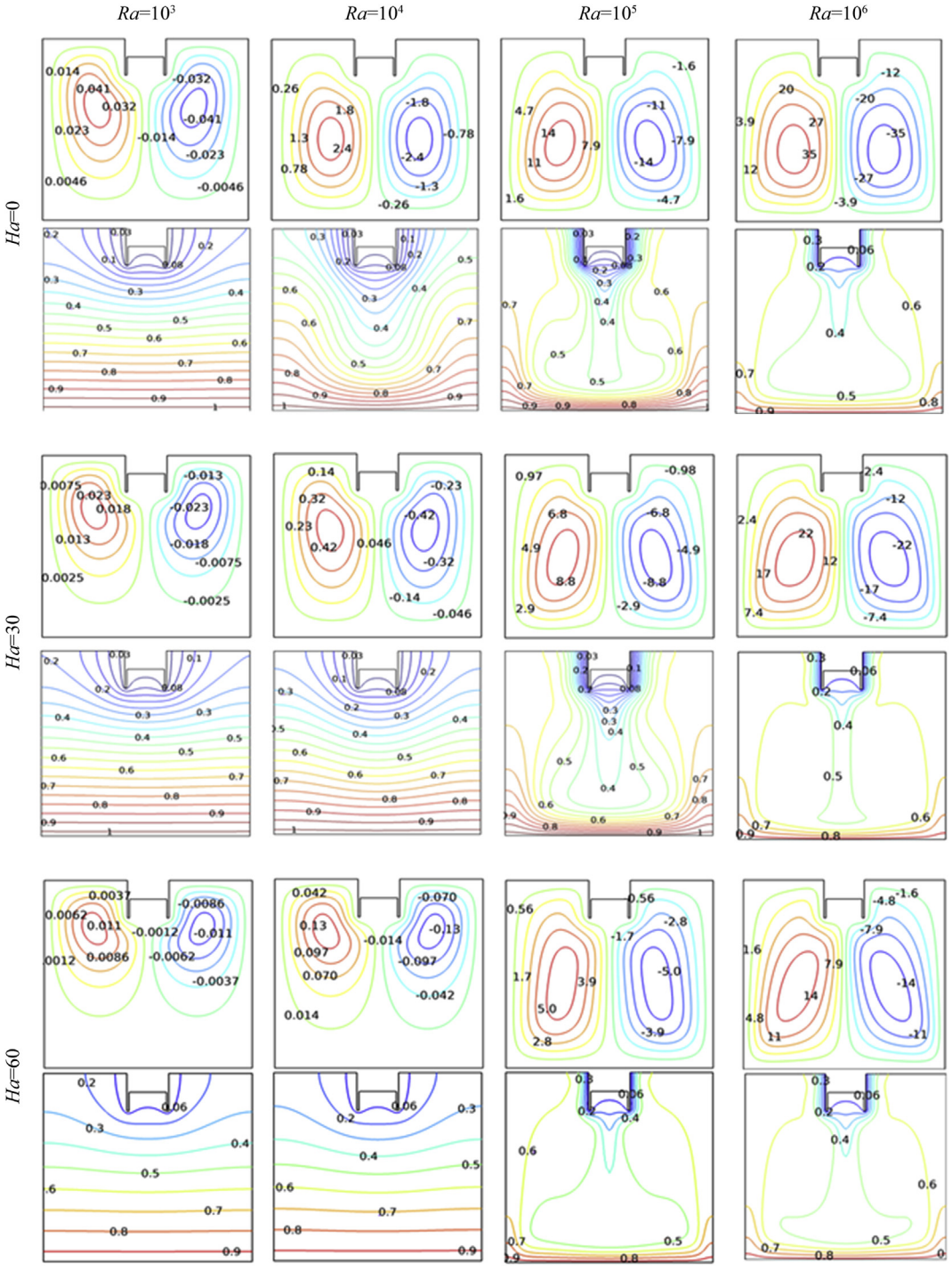

Figure 4 Influence of Rayleigh number *Ra* and Hartmann number *Ha* on streamlines and isotherms at nanoparticle volume fraction $\phi = 0.04$.

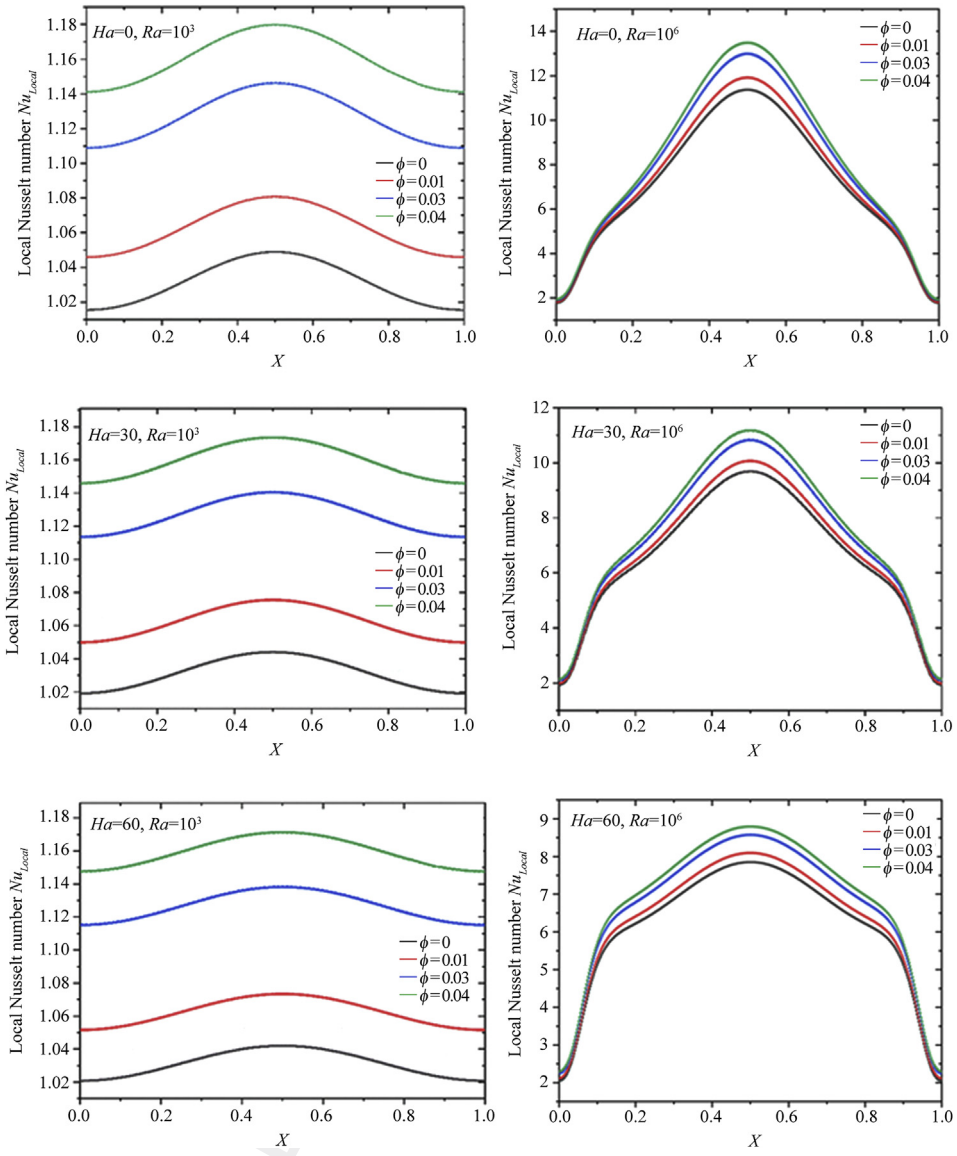

Figure 5 Variation of local Nusselt number Nu_{Local} along the hot surface for different nanoparticle volume fractions ϕ.

field. The Nusselt number of Cu−H_2O ($\phi = 4\%$) with $Ra = 10^6$, the fore-mentioned elements to extend an understanding of the grid finesse as publicized in Table 2. There is no significant alter of average Nusselt number after the elements of 5929. Therefore, all computations are made for this size.

Figure 2 presents the variation of local Nusselt number Nu_{Local} with different Rayleigh number Ra for fixed Hartmann number $Ha = 0$. The Nu_{Local} is compared with those obtained by Ghasemi et al. [40] and found to be are in good agreement.

4. Results and discussion

This section focuses on investigating the effect of nanoparticle volume fraction (ϕ), Rayleigh number ($Ra = 10^3$ to 10^6) and Hartman number ($Ha = 0$ to 60) on the performance of magneto-hydrodynamic heat transfer in a baffled U-shaped enclosure. Figures 3 and 4 display the effect of the Rayleigh number on the fluid motion and temperature distribution inside the enclosures filled with pure fluid ($\phi = 0$) and nanofluid ($\phi = 0.04$) with ($Ha = 0$, 30 and 60) on streamlines and isotherms.

Figures 3 and 4 show two clockwise cells in the enclosure of U shape on the right and left sides of the cavity due to the presence of the baffle. One can see that the fluid near the bottom wall has become warm, and the temperature gradient enhances the buoyancy force to rise the fluid in the cavity. Two recirculation regions have been created due the effect of the baffle. The Rayleigh number Ra leads to rise the buoyancy forces near the active wall. It can also be observed in Figures 3 and 4, for $Ra = 10^3$, that the natural conduction method is overriding. The isotherms from the baffle are horizontal. Thus, the buoyancy forces

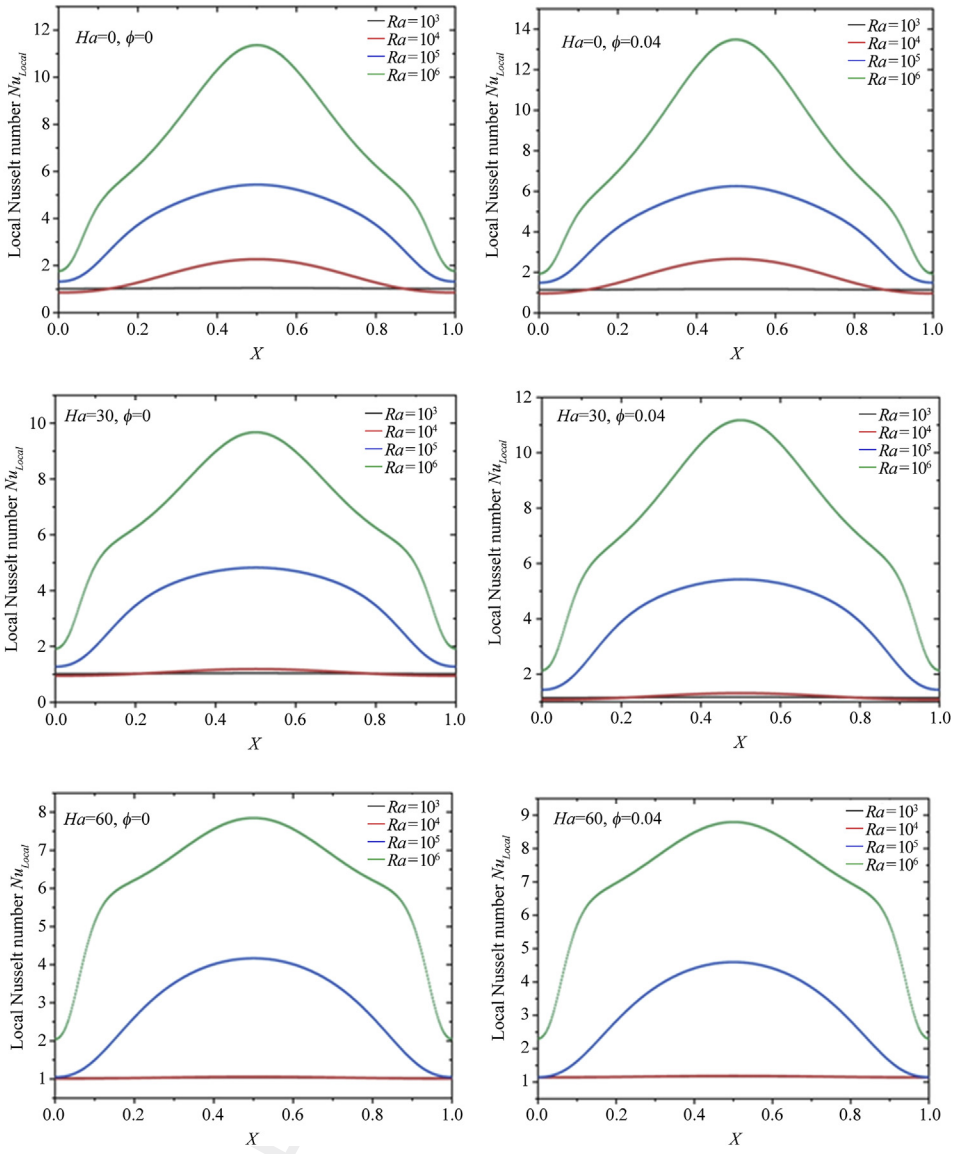

Figure 6 Variation of local Nusselt number Nu_{Local} along the hot surface for different Rayleigh numbers Ra.

created by temperature gradient leads to up were the fluid in the cavity. It can be seen that for increasing Rayleigh number Ra from 10^3 to 10^4 there is no significant change on the isotherms. As for $Ra = 10^5$, the results show the appearance of a thermal plume near the U-shaped enclosure and the baffle. In addition to two stronger clockwise cells, it is because of convective heat transport [41–44]. For Hartmann number Ha equal to 60 the thermal plume become weakness.

Figures 5 and 6 show the effect of the Rayleigh number Ra, Hartmann number Ha, and nanoparticles concentration ϕ on local Nusselt number (Nu_{Local}) along the hot bottom wall. As the volume fraction of nanofluid increases, flow and heat transfer characteristics are enhanced due to an increase in fluid flow by adding Cu concentration. As shown in Figure 5, the variation of Nu_{Local} is independent of the values of both the Hartmann and the Rayleigh numbers. The former always increases reaching a peak value then diminishes along the bottom wall. The position of the peak value indicates the cause of the baffle on increasing the Nusselt number and it can be located by projecting the position of the baffle on the bottom wall. At low Rayleigh numbers (10^3), the effect of Rayleigh number on heat transfer rate is unapparent due to the dominated conduction heat transfer.

However, at $Ra = 10^4$ the four lines of the Hartmann number differ from each other revealing that when increasing the Hartmann number, the Nusselt number neighboring to the baffle declined slightly. The both sides of the bottom wall are located far away from the baffle, their Nusselt number increases. Finally, at $Ra = 10^5$, there is significant variation of the Nusselt number as a function of the Ha. In this case, when increasing the Ha from zero to 60, there are two different variations of the corresponding

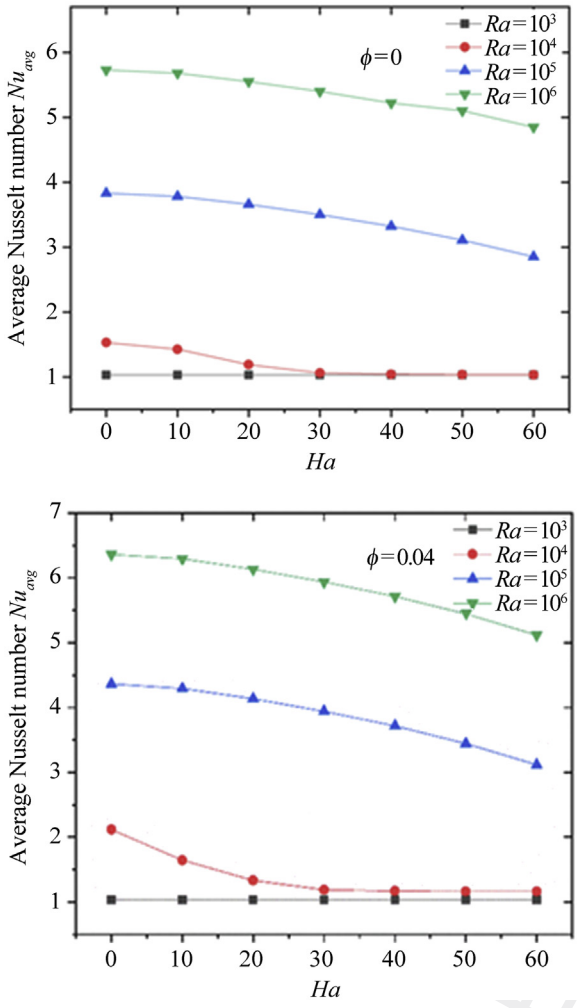

Figure 7 Variation of average Nusselt number along bottom wall for $\phi = 0.01$ and 0.04.

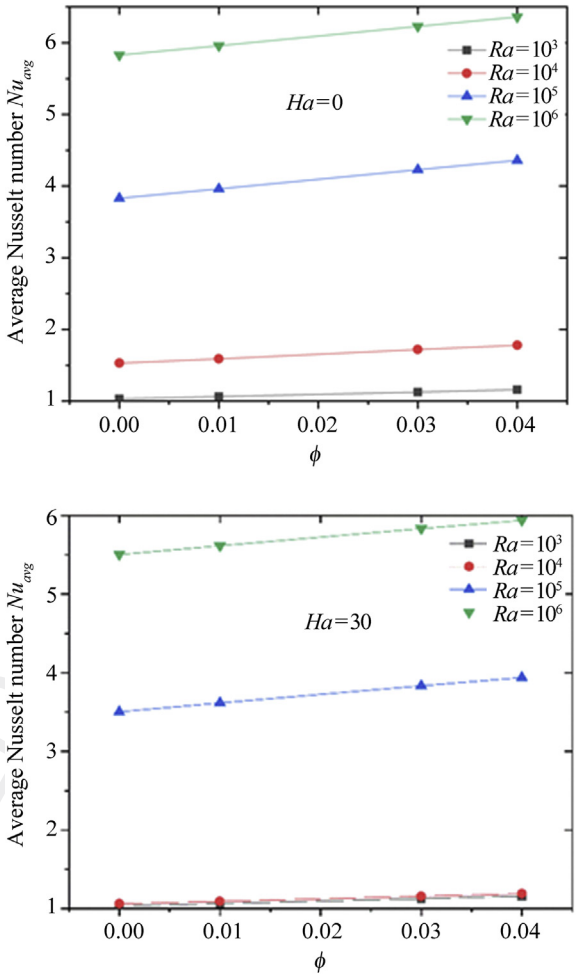

Figure 8 Variation of average Nusselt number for different nanoparticle volume fraction for $Ha = 0$ and $Ha = 30$.

Nusselt number. It first decreases on each node of the bottom wall in the interval from zero to 30, and then it increases in the interval from 30 to 60 despite that the local Nusselt number increases on most nodes on the bottom wall.

Figure 7 demonstrates the deviation of average Nusselt number for different Rayleigh number Ra of bottom wall as a function of the Hartmann number Ha in two cases ($\phi = 0$ and $\phi = 0.04$).

As shown in Figure 7, the average Nusselt number has a completely different behavior. It is simply a constant at $Ra = 10^3$ if the Hartmann number is decreased, however beyond the value $Ra = 10^4$, it decreases if the Hartmann number is increased. These variations are because the magnetism has almost no effect on heat transfer in the first case ($Ra = 10^3$) and it weaken the convection mode in the second case ($Ra > 10^4$). In the former case, the variation of heat transfer is due solely to the conduction. As depicted in Figure 8, the Nusselt number has a monotonic increasing as a function of ϕ. This is because the insertion of nanoparticles enlarges thermal conductivity with the increase of energy transport.

The deviation of the average Nusselt number as a function of the Ra and Ha for different values of ϕ are depicted in Figure 8. The curves show a strong increase of the Nusselt number when the Ra is increased in the interval $Ra = 10^4$ to $Ra > 10^5$. In general, the average Nusselt number is augmented with ϕ. In addition, as Rayleigh numbers increase the average Nusselt number is similarly increasing. At low Rayleigh number (Ra), the effect of nanoparticle is more pronounced due to conduction dominating the heat transfer.

5. Conclusions

In this paper, we have studied the natural convection of Cu−H_2O nanoliquids under magnetism in a baffled U-shaped enclosure. The results are displayed in the forms of isotherms, streamlines and Nusselt number profiles. At low value of the Rayleigh number the system is in conduction dominated regime and this leads to a vertical isotherm stratification and weak circulation in the cavity. When mounting the Rayleigh number, convection becomes the principal mechanism for heat transport. As a results a strong thermal gradient establishes

approximately the vertical wall of the cavity and it increases when mounting the Rayleigh number or diminishing the Hartmann number. From analyzing the simulation data for the average of the Nusselt number, we found that the nanoparticle volume fraction has strong effect of heat transport on a nanoliquid, which increases remarkably due to increase of the volume fraction. For $Ra = 10^3$ and $Ra = 10^4$, Hartmann effects only weakly the heat transfer because the magnetic field suppresses convection flow. Due to this, the average Nusselt number unaltered with Hartmann number. The average Nusselt number augmented when decreasing the nanoparticle volume fraction. This happens in the regime where $Ra > 10^5$ and $Ha > 20$.

Acknowledgements

This research was supported by the Algerian Ministry of Higher Education and Scientific Research through PRFU project no B00L02UN210120180002, and the General Directorate of Scientific Research and Technological Q4 Development, Algeria (DGRSDT).

References

[1] M. Sheikholeslami, M.M. Rashidi, Effect of space dependent magnetic field on free convection of Fe_3O_4-water nanofluid, J. Taiwan Inst. Chem. Eng. 56 (2015) 6−15, https://doi.org/10.1016/j.jtice.2015.03.035.

[2] F. Garoosi, L. Jahanshaloo, M.M. Rashidi, A. Badakhsh, M.E. Ali, Numerical simulation of natural convection of the nanofluid in heat exchangers using a Buongiorno model, Appl. Math. Comput. 254 (2015) 183−203, https://doi.org/10.1016/j.amc.2014.12.116.

[3] M. Sathiyamoorthy, A.J. Chamkha, Effect of magnetic field on natural convection flow in a liquid gallium filled square cavity for linearly heated side wall(s), Int. J. Therm. Sci. 49 (9) (2010) 1856−1865, https://doi.org/10.1016/j.ijthermalsci.2010.04.014.

[4] A.H. Mahmoudi, M. Shahi, R. Abbas Honarbakhsh, A. Ghasemian, Numerical study of natural convection cooling of horizontal heat source mounted in a square cavity filled with nanofluid, Int. Commun. Heat Mass Tran. 37 (8) (2010) 1135−1141, https://doi.org/10.1016/j.icheatmasstransfer.2010.06.005.

[5] F. Mebarek-Oudina, Convective heat transfer of Titania nanofluids of different base fluids in cylindrical annulus with discrete heat source, Heat Tran. Asian Res. 48 (2019) 135−147.

[6] N.M. Al-Najem, K.M. Khanafer, M.M. El-Refaee, Numerical study of laminar natural convection in tilted enclosure with transverse magnetic field, Int. J. Numer. Methods Heat Fluid Flow 8 (1998) 651−672, https://doi.org/10.1108/09615539810226094.

[7] U. Khan, A. Zaib, F. Mebarek-Oudina, Mixed convective magneto flow of SiO_2-MoS_2/$C_2H_6O_2$ hybrid nanoliquids through a vertical stretching/shrinking wedge: stability analysis, Arabian J. Sci. Eng. Q5 (2020), https://doi.org/10.1007/s13369-020-04680-7.

[8] H.F. Öztop, M.M. Rahman, A. Ahsan, M. Hasanuzzaman, R. Saidur, K. Al-Salem, N.A. Rahim, MHD natural convection in an enclosure from two semi-circular heaters on the bottom wall, Int. J. Heat Mass Tran. 55 (7−8) (2012) 1844−1854.

[9] S. Marzougui, F. Mebarek-Oudina, A. Aissa, M. Magherbi, Z. Shah, K. Ramesh, Entropy generation on magneto-convective flow of copper-water nanofluid in a cavity with chamfers, J. Therm. Anal. Calorim. (2020), https://doi.org/10.1007/s10973-020-09662-3.

[10] A. Zaim, A. Aissa, F. Mebarek-Oudina, A.M. Rashad, M.A. Hafiz, M. Sahnoun, M. El Ganaoui, Magnetohydrodynamic natural convection of hybrid nanofluid in a porous enclosure: numerical analysis of the entropy generation, J. Therm. Anal. Calorim. 141 (5) (2020) 1981−1992.

[11] S.A.M. Mehryan, M.A. Sheremet, M. Soltani, M. Izadi, Natural convection of magnetic hybrid nanofluid inside a double-porous medium using two-equation energy model, J. Mol. Liq. 277 (2019) 959−970, https://doi.org/10.1016/j.molliq.2018.12.147.

[12] M. Alkasassbeh, Z. Omar, F. Mebarek-Oudina, J. Raza, A.J. Chamkha, Heat transfer study of convective fin with temperature-dependent internal heat generation by hybrid block method, Heat Tran. Asian Res. 48 (4) (2019) 1225−1244.

[13] A.I. Alsabery, T. Armaghani, A.J. Chamkha, Conjugate heat transfer of Al_2O_3-water nanofluid in a square cavity heated by a triangular thick wall using Buongiorno's two-phase model, J. Therm. Anal. Calorim. (2018) 1−16, https://doi.org/10.1007/s10973-018-7473-7.

[14] S. Hamrelaine, F. Mebarek-Oudina, M.R. Sari, Analysis of MHD Jeffery Hamel flow with suction/injection by homotopy analysis method, J. Adv. Res. Fluid Mech. Therm. Sci. 58 (2) (2019) 173−186.

[15] J. Raza, F. Mebarek-Oudina, A.J. Chamkha, Magnetohydrodynamic flow of molybdenum disulfide nanofluid in a channel with shape effects, Multidiscip. Model. Mater. Struct. 15 (4) (2019) 737−757.

[16] F. Mebarek-Oudina, R. Bessaih, B. Mahanthesh, A.J. Chamkha, J. Raza, Magneto-thermal-convection stability in an inclined cylindrical annulus filled with a molten metal, Int. J. Numer. Methods Heat Fluid Flow (2020), https://doi.org/10.1108/HFF-05-2020-0321.

[17] K. Swain, B. Mahanthesh, F. Mebarek-Oudina, Heat transport and stagnation-point flow of magnetized nanoliquid with variable thermal conductivity with Brownian moment and thermophoresis aspects, Heat Transfer (2020), https://doi.org/10.1002/htj.21902.

[18] J. Raza, M. Farooq, F. Mebarek-Oudina, B. Mahanthesh, Multiple slip effects on MHD non-Newtonian nanofluid flow over a nonlinear permeable elongated sheet, Multidiscip. Model. Mater. Struct. 15 (5) (2019) 913−931.

[19] J. Raza, F. Mebarek-Oudina, P. Ram, S. Sharma, MHD flow of non-Newtonian molybdenum disulfide nanofluid in a converging/diverging channel with Rosseland radiation, Defect Diffusion Forum 401 (2020) 92−106, https://doi.org/10.4028/www.scientific.net/DDF.401.92.

[20] G.T. Liang, I. Mudawar, Review of single-phase and two-phase nanofluid heat transfer in macro-channels and micro-channels, Int. J. Heat Mass Tran. 136 (2019) 324−354.

[21] M. Akbari, N. Galanis, A. Behzadmehr, Comparative analysis of single and two-phase models for CFD studies of nanofluid heat transfer, Int. J. Therm. Sci. 50 (2011) 1343−1354.

[22] M. Sheikholeslami, D.D. Ganji, Y.M. Javed, R. Ellahi, Effect of thermal radiation on magnetohydrodynamics nanofluid flow and heat transfer by means of two phase model, J. Magn. Magn Mater. 374 (2015) 36−43.

[23] H. Sayehvand, A. Habibzadeh, A. Mekanik, CFD analysis of natural convection heat transfer in a square cavity with partitions utilizing Al_2O_3 nanofluid, Int. J. Nano Dimens. (IJND) (2012) 191−200, https://doi.org/10.7508/IJND.2011.03.007.

[24] M.A. Medebber, A. Aissa, M.A. Slimani, N. Retiel, Numerical study of natural convection in vertical cylindrical annular enclosure filled with Cu-water nanofluid under magnetic fields, Defect Diffusion Forum 392 (2019) 123−137, https://doi.org/10.4028/www.scientific.net/DDF.392.123.

[25] P. Kandaswamy, J. Lee, A.K. Abdul Hakeem, S. Saravanan, Effect of baffle-cavity ratios on buoyancy convection in a cavity with mutually orthogonal heated baffles, Int. J. Heat Mass Tran. 51 (7−8) (2008) 1830−1837, https://doi.org/10.1016/j.ijheatmasstransfer.2007.06.039.

[26] T. Armaghani, A. Kasaeipoor, N. Alavi, M.M. Rashidi, Numerical investigation of water-alumina nanofluid natural convection heat transfer and entropy generation in a baffled L-shaped cavity, J. Mol. Liq. 223 (2016) 243−251.

[27] Y. Ma, R. Mohebbi, M.M. Rashidi, Z.G. Yang, M.A. Sheremet, Numerical study of MHD nanofluid natural convection in a baffled U-

shaped enclosure, Int. J. Heat Mass Tran. 130 (2019) 123−134, https://doi.org/10.1016/j.ijheatmasstransfer.2018.10.072.
[28] Z.Q. Zuo, W.B. Jiang, Y.H. Huang, Effect of baffles on pressurization and thermal stratification in cryogenic tanks under micro-gravity, Cryogenics 96 (2018) 116−124.
[29] S. Saravanan, A.R. Vidhya, Natural convection in square cavity with heat generating baffles, Appl. Math. Comput. 244 (2014) 1−9, https://doi.org/10.1016/j.amc.2014.06.092.
[30] Y. Ma, R. Mohebbi, M.M. Rashidi, O. Manca, Z.G. Yang, Numerical investigation of MHD effects on nanofluid heat transfer in a baffled U-shaped enclosure using lattice Boltzmann method, J. Therm. Anal. Calorim. 135 (6) (2019) 3197−3213.
[31] H. Benzenine, R. Saim, S. Abboudi, O. Imine, Numerical simulation of the dynamic turbulent flow field through a channel provided with baffles: comparative study between two models of baffles: transverse plane and trapezoidal, Revue Ener. Renouvel. 13 (4) (2010) 639−651.
[32] A. Chamkha, M. Ismael, A. Kasaeipoor, T. Armaghani, Entropy generation and natural convection of CuO-water nanofluid in C-shaped cavity under magnetic field, Entropy 18 (2) (2016) 50, https://doi.org/10.3390/e18020050.
[33] H.C. Brinkman, The viscosity of concentrated suspensions and solutions, J. Chem. Phys. 20 (4) (1952) 571, https://doi.org/10.1063/1.1700493.
[34] B.C. Pak, Y.I. Cho, Hydrodynamic and heat transfer study of dispersed fluids with submicron metallic oxide particles, Exp. Heat Tran. 11 (2) (1998) 151−170, https://doi.org/10.1080/08916159808946559.
[35] K.U. Rehman, M.Y. Malik, M. Zahri, Q.M. Al-Mdallal, M. Jameel, M.I. Khan, Finite element technique for the analysis of buoyantly convective multiply connected domain as a trapezium enclosure with heated circular obstacle, J. Mol. Liq. 286 (2019) 110892, https://doi.org/10.1016/j.molliq.2019.110892.
[36] D. Jean, A. Huerta, Finite Element Methods for Flow Problems, John Wiley & Sons, 2003.
[37] P. Nithiarasu, R.W. Lewis, K.N. Seetharamu, Fundamentals of the Finite Element for Heat and Mass Transfer, John Wiley & Sons, 2016.
[38] F. Mebarek-Oudina, Numerical modeling of the hydrodynamic stability in vertical annulus with heat source of different lengths, Eng. Sci. Technol. 20 (4) (2017) 1324−1333, https://doi.org/10.1016/j.jestch.2017.08.003.
[39] M. Farhan, Z. Omar, F. Mebarek-Oudina, J. Raza, Z. Shah, R.V. Choudhari, O.D. Makinde, Implementation of one step one hybrid block method on nonlinear equation of the circular sector oscillator, Comput. Math. Model. 31 (1) (2020) 116−132.
[40] B. Ghasemi, S.M. Aminossadati, A. Raisi, Magnetic field effect on natural convection in a nanofluid-filled square enclosure, Int. J. Therm. Sci. 50 (9) (2011) 1748−1756.
[41] F. Mebarek-Oudina, A. Aissa, B. Mahanthesh, H.F. Öztop, Heat transport of magnetized Newtonian nanoliquids in an annular space between porous vertical cylinders with discrete heat source, Int. Commun. Heat Mass Tran. 141 (2) (2020) 104737, https://doi.org/10.1016/j.icheatmasstransfer.2020.104737.
[42] S. Gourari, F. Mebarek-Oudina, A.K. Hussein, L. Kolsi, W. Hassen, O. Younis, Numerical study of natural convection between two co-axial inclined cylinders, Int. J. Heat Tech. 37 (3) (2019) 779−786.
[43] H. Laouira, F. Mebarek-Oudina, A.K. Hussein, L. Kolsi, A. Merah, O. Younis, Heat transfer inside a horizontal channel with an open trapezoidal enclosure subjected to a heat source of different lengths, Heat Tran. Asian Res. 49 (1) (2020) 406−423, https://doi.org/10.1002/htj.21618.
[44] F. Mebarek-Oudina, N. Keerthi Reddy, M. Sankar, Heat source location effects on buoyant convection of nanofluids in an annulus, in: B. Rushi Kumar, R. Sivaraj, J. Prakash (Eds.), Advances in Fluid Dynamics, 2020, pp. 923−937, https://doi.org/10.1007/978-981-15-4308-1_70.